

Deliverable 16:

**A comprehensive regional monitoring system:
monitoring strategies for climate change, N/P/Si changes,
HABs (Harmful algal blooms), and jellyfish blooms**

National Marine Environmental Monitoring Center

2019.11

A comprehensive regional monitoring system: monitoring strategies for climate change, N/P/Si changes, HABs (Harmful algal blooms), and jellyfish blooms

1. Introduction

As the YSLME project defined, the Yellow Sea is the semi-enclosed body of water bounded as follows: to the west by the Chinese mainland south of Penglai and a line from Penglai to Dalian; to the east by the Korean Peninsula and Cheju Island and a line drawn from Jindo Island off the south coast of the Korean mainland to the north coast of Cheju Island; and to the south by a line running from the north bank of the mouth of the Yangtze River (Chang Jiang) to the southwestern coast of Cheju Island.

1.1 Climate change

Yellow Sea Cold Water Mass (YSCWM) is a unique hydrographic phenomenon in the Yellow Sea. This water mass is located in the central trough of the Yellow Sea. In spring increased solar radiation heats the Yellow Sea, but the water in the central trough, which is a remnant of cold, vertically well mixed water in the previous winter, remains cold because of the depth. As temperature gradient around the water becomes greater in spring through summer, the water is distinctively seen as a dome on the trough. The strong temperature gradient prevents the heat transfer from the surrounding so that the water can remain cold until breaking down in early winter (November). This cold water, because it is more noticeable in the temperature field, is called the Yellow Sea Cold Water Mass (YSCWM) in many literature (Fig.1-1).

Since YSCWM is the most conservative among water masses in the Yellow Sea, it influences catches and fishing grounds of demersal fishes. YSCWM serves as an overwintering site for many temperate species. The intensity of summer southward/southeastward migration of YSCWM including the cold water over the eastern Yangtze Bank affects the upstream path of the Tsushima Warm Current, and

eventually induces changes in the regional hydrography in the southern Yellow Sea and the northern East China Sea.

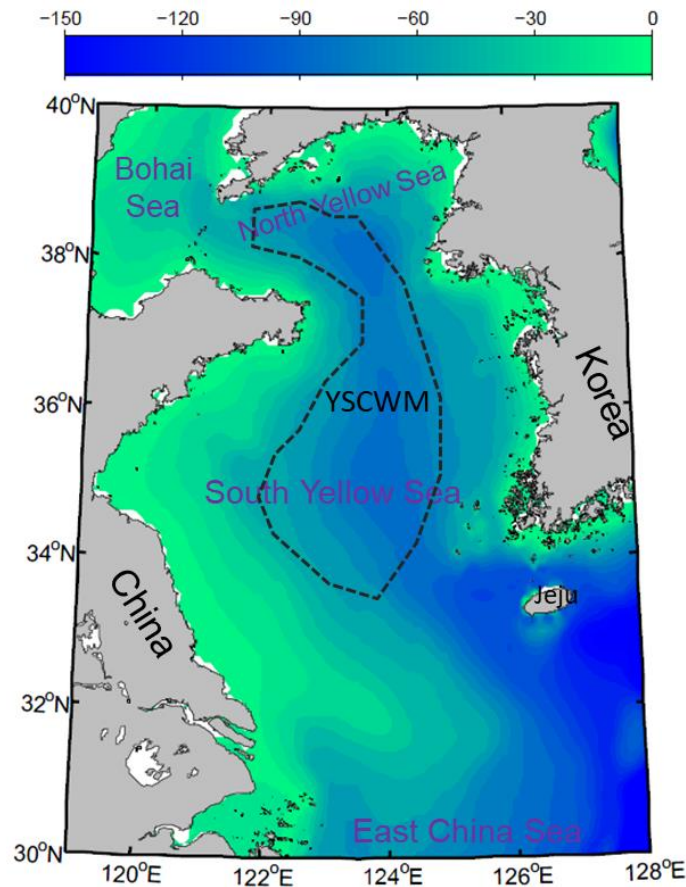


Fig. 1-1 Geography and location of YSCWM. Area with temperature at 50m colder than 11°C in August were selected as the YSCWM region.

1.1.1 Sea surface temperature changes in the YSCWM region

Based on a set of seasonally monitored data along the transect (at 36°N) maintained by the State Oceanic Administration of China, an ascending trend was found in sea surface temperature in the Yellow Sea (Fig. 1-2). The annual mean rates of change were between 0.038 and 0.094 °C. The regional mean of water column average temperature increased 1.7 °C during the observation period. This increase is significant. The warming of seawater in the Yellow Sea during 1976–2000 is consistent with the

increase in the mean air temperature observed throughout northern China and the increase in SST found in both the Bohai Sea and the East China Sea.

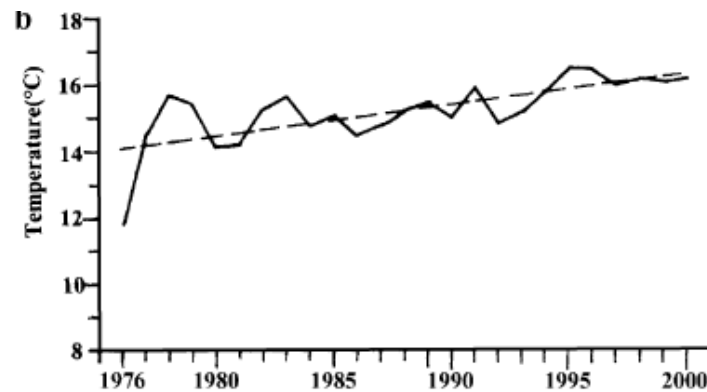


Fig. 1-2 Sea surface temperature changes in the Yellow Sea (36°N transect data, Lin et al, 2005)

SST anomaly time-series of the KODC dataset at 125°E, 35.9°N and the global dataset at 124°E, 36.0°N were also examined in Park et al (2011). The global SST anomaly varies at a smaller extent because of differences in observation methods and preprocesses between the two datasets, whereas the KODC SST anomaly shows larger variability: the KODC SST is ~1.5 °C higher (lower) in August (February and April) than the global SST (Fig. 1-3a). However, the similarity in the long term variation trend between the two time-series is perceived by the undulating peaks of them. This similarity is more evident in the time series of spatially-averaged non-seasonal SST anomaly (Fig. 1-3b). Another global dataset, International Comprehensive Ocean-atmosphere Data Set (ICOADS), shows the similar features as well. Since the seasonal cycle was deleted, the range of the variability is almost the same, -1.2 °C to 1.4 °C, among the three time-series. Although the KODC time-series retains more short-term features, the three datasets are consistent in the long-term scales such as inter-annual to inter-decadal scales with the correlation coefficient of 0.8.

The variability of YSCWM is usually represented by the temperature at bottom layers, such as 50m depth, to avoid the seasonal variation. The results in Park et al (2011) showed YSCWM revealed three cold events (1967–1971, 1983–1988 and 1996–2006)

and two warm events (1972–1980 and 1990–1995), although the anomaly is little weak during 1990–1995. A relationship was also found between upper and bottom layers in summer: warm (cold) anomaly appears in the upper (bottom) layer in June/August during the cold (warm) events. In the cold events, as the increased vertical temperature gradient of the thermocline impedes the downward heat transfer, the warming of YSCWM which peaks from June to August slows down in comparison with the normal years. In the warm events an opposite scenario occurs. Moreover, since the remnant of the winter Yellow Sea Warm Current Water remains in the Yellow Sea trough, YSCWM can be influenced by variability of the Yellow Sea Warm Current. Taking the Pacific Decadal Oscillation into account, the Yellow Sea Warm Current might be the last pathway that the Pacific Decadal Oscillation is transferred through the Kuroshio to the Yellow Sea.

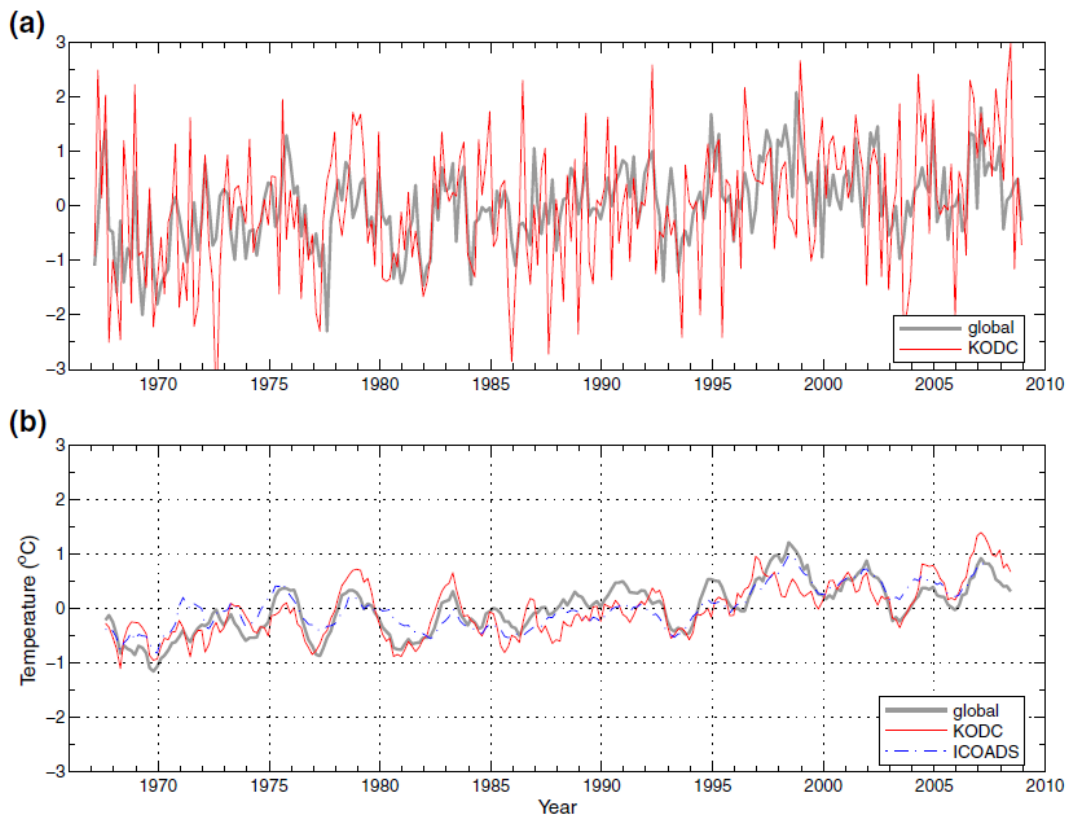


Fig. 1-3 SST anomaly time-series in the YSCWM from KODC (125°E, 35.9°N), global (124°E, 36.0°N; nearest to the KODC data location), and ICOADS: (a) before removing the seasonal cycle and (b) after removing the seasonal cycle. (Park et al, 2011)

1.1.2 Structure of plankton communities in the YSCWM region

Net samples data from two co-operative cruises in the YSLME are used here to show the characteristics of plankton communities in the Yellow Sea. These two cruises were carried out in the Southern Yellow Sea in 2008, one in winter (17 to 31 January) and another in summer (2 to 13 August). Detailed sampling methods have been described in the UNDP/GEF cruises report (2011).

1.1.2.1 Phytoplankton

There were a total of 62 and 139 species of phytoplankton identified in winter and summer, respectively. In winter, the number of dominant species is much more than that in summer (Table 1-1). *Chaetoceros lorenzianus* and *Pseudonitzschia pungens* are the common dominant species in both seasons.

Table 1-1. Dominant species of net phytoplankton samples in in 2011

Winter		Summer	
Species	Dominance	Species	Dominance
<i>Corethron hystrix</i>	0.051	<i>Chaetoceros lorenzianus</i>	0.239
<i>Chaetoceros densus</i>	0.039	<i>Chaetoceros</i> spp.	0.039
<i>Ditylum brightwelli</i>	0.032	<i>Chaetoceros affinis</i>	0.030
<i>Chaetoceros lorenzianus</i>	0.029	<i>Chaetoceros pseudocurvisetus</i>	0.013
<i>Coscinodiscus oculus-iridis</i>	0.028	<i>Pseudonitzschia pungens</i>	0.010
<i>Odontella sinensis</i>	0.028		
<i>Bacillaria pacillifera</i>	0.025		
<i>Coscinodiscus wailesii</i>	0.016		
<i>Ceratium intermedium</i>	0.015		

<i>Coscinodiscus</i> sp.	0.015
<i>Pseudonitzschia pungens</i>	0.013
<i>Guinardia flaccida</i>	0.013
<i>Coscinodiscus asteromphalus</i>	0.010

In the net samples collected in winter, several diatoms dominated with similar dominance indexes. For example, the abundance of *Corethron hystrix* was higher in the north than that in the south, while *Chaetoceros densus* showed high density in the central zone and was not found in the southeast part of the study area (Fig. 1-4).

In the summer net samples, the genus *Chaetoceros* was the most dominant taxon with an average of 632×10^4 cells/m³, and accounted for 87.8% of total abundance. It defined the horizontal distribution features of phytoplankton abundance, i.e., the overall distribution pattern showed higher values in the southwest and low values in most other parts (Fig. 1-5). *Chaet lorenzianus* was the most dominant species, averaging 374×10^4 cells/m³, and accounting for 52% of the total abundance. This species shaped the main features of total abundance in the net samples.

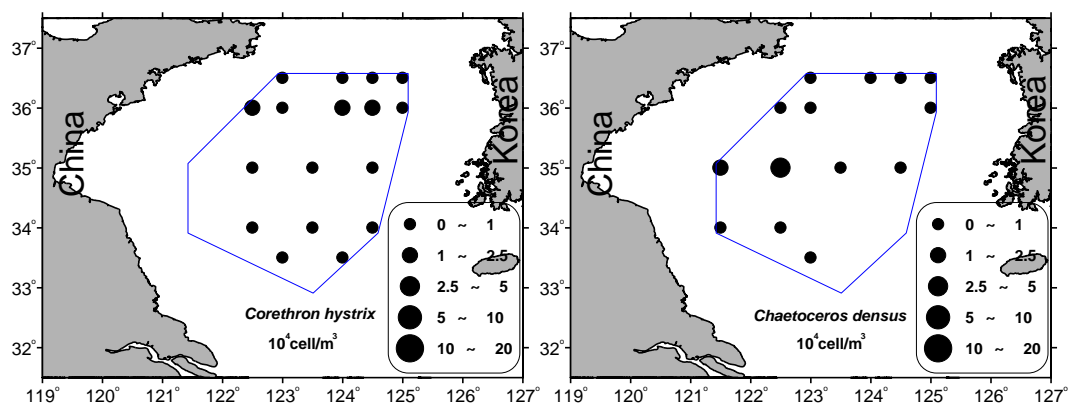


Fig. 1-4. Distribution of *Corethron hystrix* (left) and *Chaetoceros densus* (right) in net samples in winter.

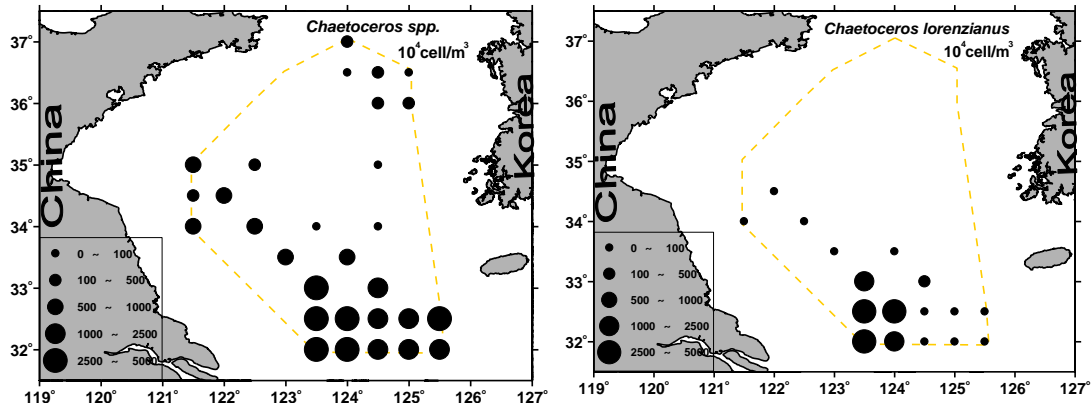


Fig. 1-5. Distribution of *Chaetoceros* spp. (left) and *C. lorenzianus* (right) in the summer net samples.

Net sampled phytoplankton species diversity (H') in winter varied between 0.22-4.24. The highest diversity occurred at the stations with high cell abundance (southwest zone). In general, the species diversity indexes of phytoplankton were higher in the south as compared to the north (Fig. 1-6, left panel). In the summer, the diversity of net samples scored from 0.19-3.84 with a mean value of 1.87. Low levels of diversity were found in the southeast and northwest (Fig. 1-6, right panel).

1.1.2.2 Zooplankton

Data from the samples collected with the 505 μm mesh plankton net were used here to show the zooplankton community structure. In winter, a total of 71 zooplankton species (otherwise lowest taxonomy level) were identified, including copepods (26 species), larvae (18 species), mysidacea (6 species), medusa (5 species),

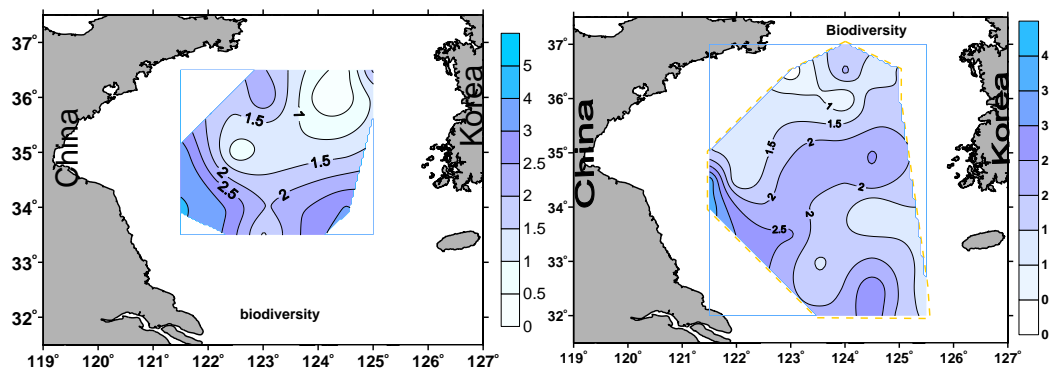


Fig. 1-6. Species diversity (H') of phytoplankton community in winter (left) and summer (right).

mastigopus (3 species), chaetognaths (2 species), euphausiids (2 species), and other

groups. In summer, a total of 77 zooplankton species were identified, including copepods (37 species), medusa (11 species), mysids (9 species), tunicates (4 species), pteropods (3 species), decapods (3 species), and other groups. The survey results showed that *Calanus sinicus* and *Sagitta crassa* were the main dominant species in the YSCWM area, and the composition of dominant species was similar between winter and summer (Table 1-2).

In winter, *Sagitta crassa* was the most abundant specie, and its abundance varied between 4 and 202 ind./m³ (mean: 98 ind./m³). There was higher abundance of *S. crassa* in the western coastal areas than that in the open sea (Fig. 1-7, left panel). The abundance of *Calanus sinicus* varied between 2 and 205 ind./m³ (mean: 37 ind/m³). There was higher abundance of *C. sinicus* in the north than that in the middle and south (Fig. 1-7, right panel).

In summer, *C. sinicus* was the most abundant species and largely contributed to total individual density. The abundance of *C. sinicus* varied from 1 to 536 ind./m³ and the magnitude was much higher (mean: 113 ind./m³) than that in winter (mean: 37 ind./m³). *C. sinicus* was evenly distributed throughout most of the study area (Fig. 1-8, left panel). The abundance of *Sagitta crassa* varied from 2 to 202 ind./m³ (mean: 40 ind./m³), and the most abundant zone was located at the west and north of the study region (Fig. 1-8, right panel).

The non-gelatinous zooplankton biomass in winter averaged 110.5 mg/m³ (in the range of 17.5-285.4 mg/m³) in the south YSCWM area, and lower biomass was found in the central and northern zones (Fig. 1-9, left panel). In summer, zooplankton biomass averaged 194.0 mg/m³ (in the range of 13.2-606.2 mg/m³), and higher biomass was found in the southeast zone (Fig. 1-9, right panel).

Table 1-2. Dominant species of net zooplankton samples in in 2011

Winter		Summer	
Species	Dominance	Species	Dominance

<i>Sagitta crassa</i>	0.383	<i>Calanus sinicus</i> **	0.467
<i>Calanus sinicus</i>	0.343	<i>Sagitta crassa</i> **	0.175
<i>Oithona plumifera</i>	0.092	<i>Oithona plumifera</i> *	0.054
<i>Parathemisto gaudichardi</i>	0.036	<i>Parathemisto gaudichardi</i>	0.048
		<i>Macrura</i> larvae	0.020

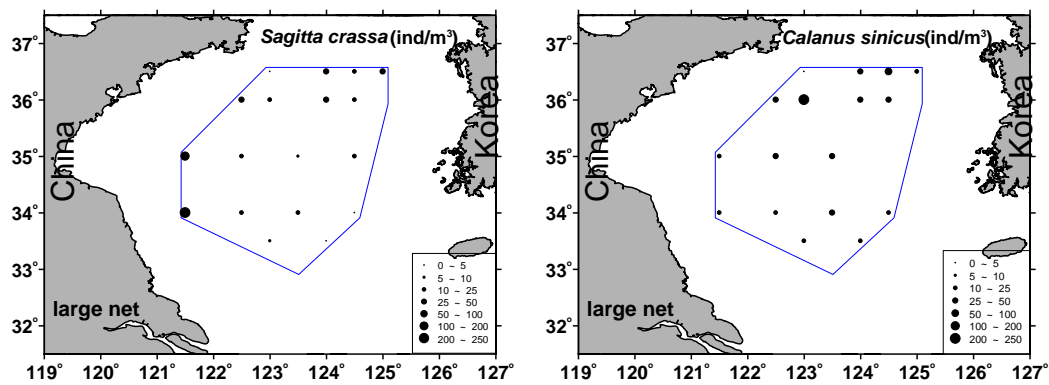


Fig. 1-7. Distribution of *Sagitta crassa* (left) and *Calanus sinicus* (right) abundance in winter.

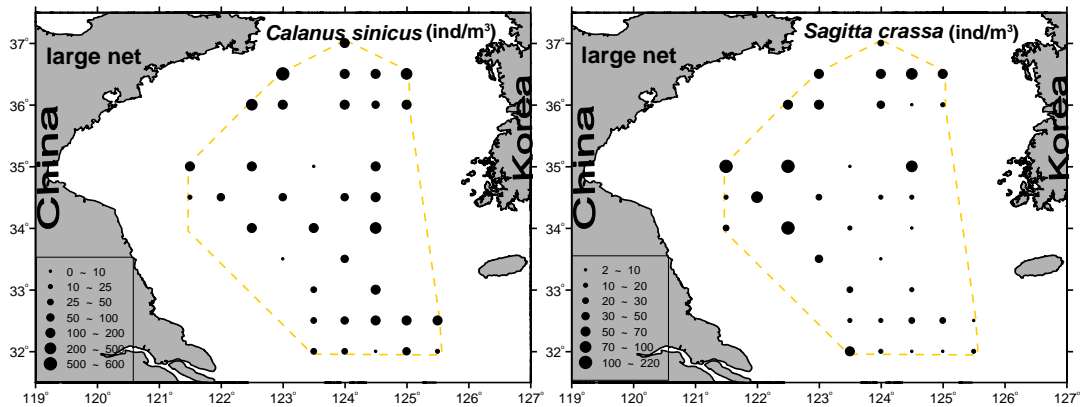


Fig. 1-8. Distribution of *Calanus sinicus* (left) and *Sagitta crassa* (right) abundance in summer.

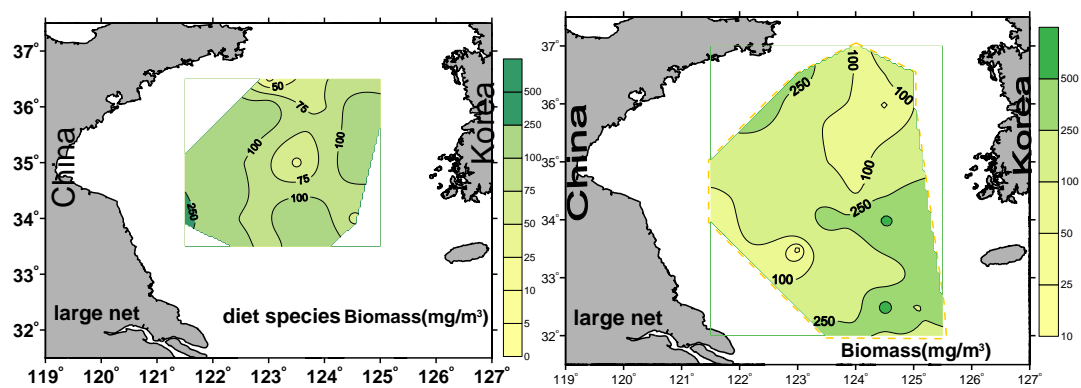


Fig. 1-9. Distribution of zooplankton biomass (mg/m^3) in winter (left) and summer (right).

In winter, the diversity index of zooplankton community was in the range of 0.64-2.87, and the lowest biodiversity was found in the west coastal areas and increasing from northwest to the southeast (Fig. 1-10, left panel). In summer, the diversity index was in the range of 0.92-3.16, and the higher biodiversity was found in the southern areas and decreasing from southwest to northeast (Fig. 1-10, right panel).

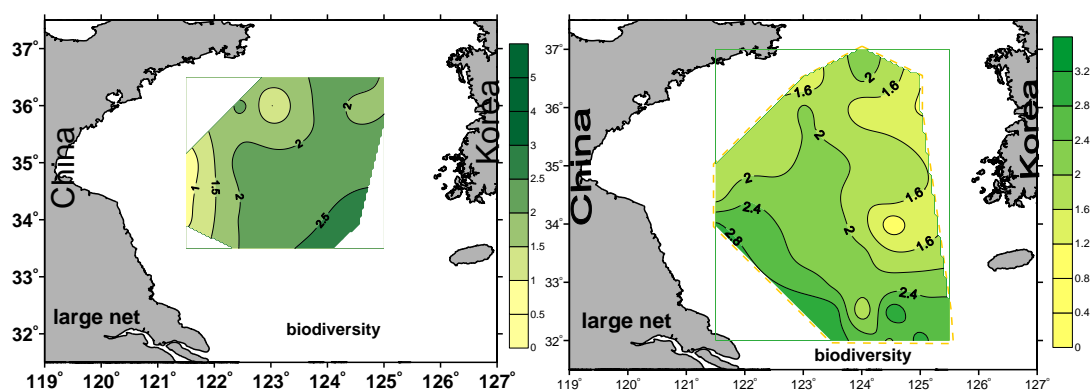


Fig. 1-10. Species diversity (H') of zooplankton community in winter (left) and summer (right).

1.1.3 Relationships between environment change and plankton community in the YSCWM region

The factors influencing plankton community in the YSCWM region are very difficult to be identified from so complex system, including many physical-chemical-biological interactions. From the trophic relationships in the marine food chains, the phytoplankton are mainly influenced by light, temperature, nutrients and herbivorous grazers in the ocean, while the zooplankton are mainly influenced by phytoplankton and nekton, through bottom-up effect of food supply and top-down control of predators.

For the temporal variation of phytoplankton, the average Chl-a concentration in the surface water of the southern Yellow Sea varied between $0.11 \text{ mg}/\text{m}^3$ and $1.62 \text{ mg}/\text{m}^3$ during 1983-2008. The Chl-a concentrations were lower in 1996–1998 as

compared to 1983–1986, followed by the suggestion of an increasing trend through at least 2007, with the highest values of the record during 2006–2007, all higher than 1 mg/m³ (Fig. 1-11). Phytoplankton cell abundance (net samples) has shown great fluctuations in the past 50 years, spanning at least 4 orders of magnitudes over the record (Fig. 1-11). The highest abundance was recorded during summer 2006 (63363×10⁴ cell m⁻³) whereas the lowest value was only 2.59×10⁴ cell m⁻³, recorded during May 2005. At present, no clear trend can be discerned in the historic dataset.

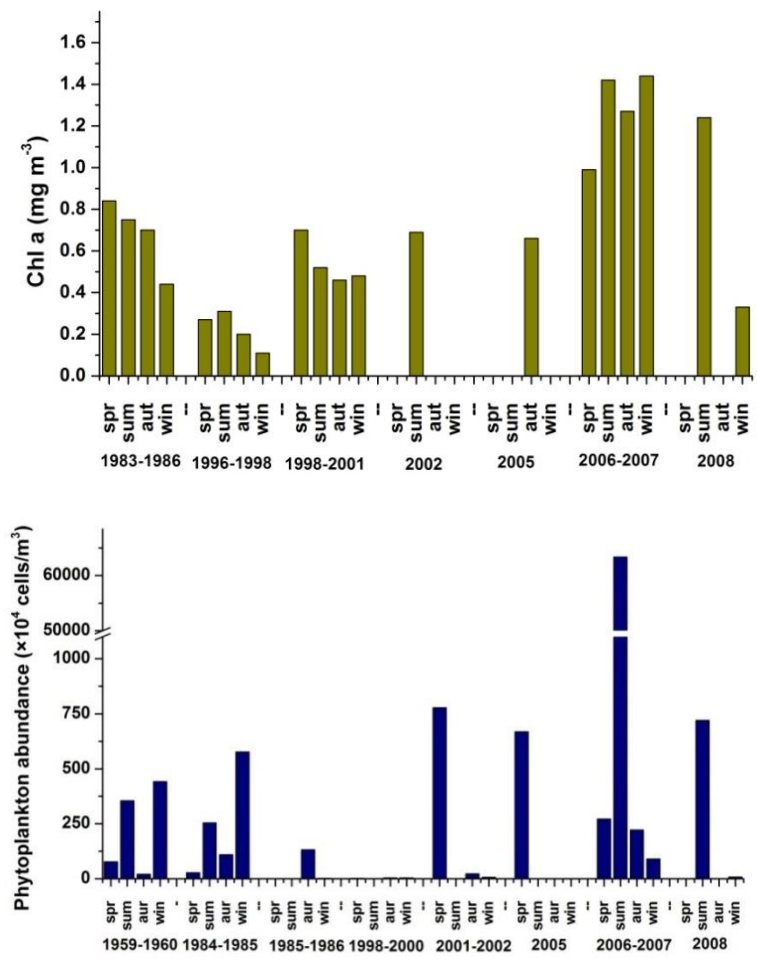


Fig. 1-11. Long term variability of chlorophyll *a* concentrations and phytoplankton abundance in southern Yellow Sea

Although the effects of temperature on diatom cell size and growth rates have been validated in laboratory cultured phytoplankton species (Montagnes and Franklin, 2001),

field results did not seem to support any obvious relationship between phytoplankton biomass and temperature. In the natural environment of ocean, temperature and nutrient are strongly covariant, the effects of temperature are more important by changing the nutrient availability rather than its direct influence on the growth of phytoplankton.

For the temporal variation of zooplankton, Liu et al (2012) suggested the seasonal pattern of the zooplankton biomass was spring and summer higher than autumn and winter in 2006-2007, which is consistent with that in 1958-1959 and 2000-2001 (Fig. 1-12). Among the long term comparison of the mean zooplankton biomass, 2006-2007 is highest, 2000-2001 comes second, 1958-1959 and 1984-1985 are relatively lowest. The zooplankton biomass has an increasing trend in recent years from the long term variability shown in Fig. 1-12. Additionally, the contribution of gelatinous zooplankton to total zooplankton biomass is much more than that of non-gelatinous zooplankton, which agrees with the frequent macro-jellyfish blooms in the Yellow Sea since the middle and later in the 1990s and even resulting in an ecological disaster in recent years.

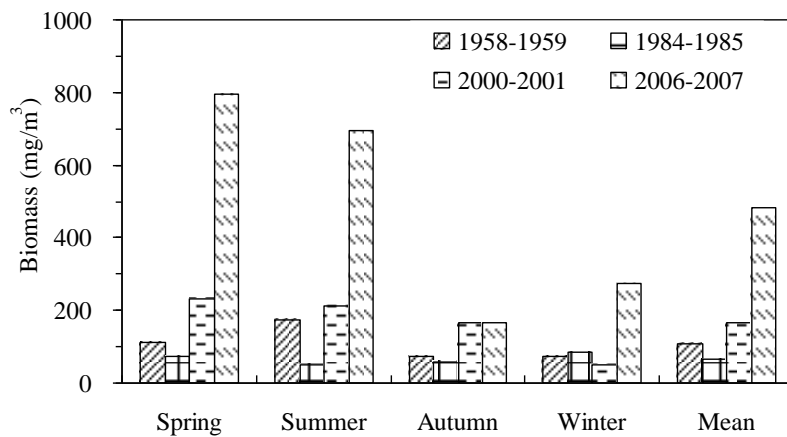


Fig. 1-12. Long term variability of the total zooplankton biomass in the southern Yellow Sea

The inter-annually seasonal variations in abundance of *Calanus sinicus* showed a significant difference between different years in the northern Yellow Sea (Fig. 1-13). The abundance of *C. sinicus* was significantly higher in 2011–2014 than that in 1959 and 1982. The overall mean abundance was 182.5 ind./m³ in 2011–2014, which was

5.5 times than that in 1959. The abundance of *C. sinicus* in 2006–2007 was also significantly higher than that in 1959 and 1982. The overall mean abundance in 2006–2007 was 191.8 ind./m³, which was 5.7 times as much as that in 1959. Further analysis shows a greater increase of its abundance in the northern YS than the southern YS and the northern ECS, suggesting a different response patterns to climate variability when compared with the subtropical seas along the Chinese coast.

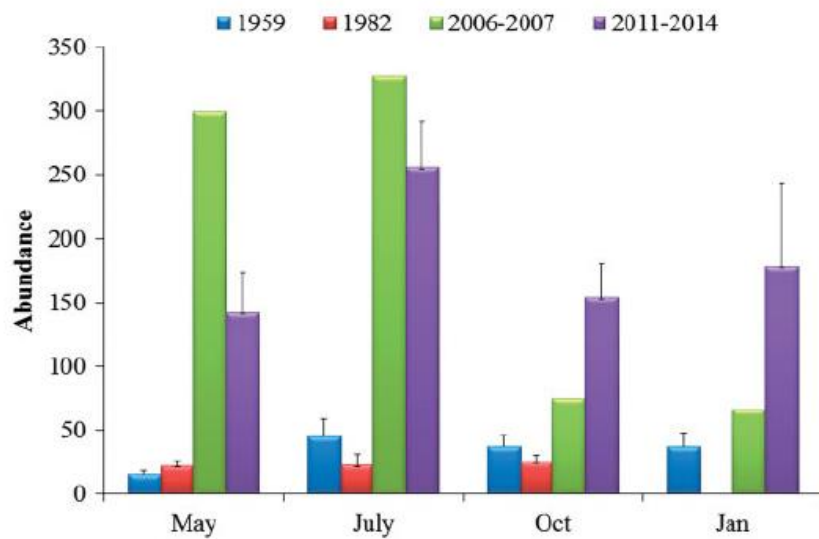


Fig. 1-13. Long term variability of *Calanus sinicus* abundance in the northern Yellow Sea

Our latest study on the phenology of seasonal phytoplankton blooms in the Yellow Sea showed also a certain relationship between temperature changes and phytoplankton dynamics. Seasonal warming and cooling may not only affect phytoplankton physiological processes but also change the stratified conditions in ways that exert controls on bloom dynamics. Relatively fast surface warming causes an earlier and stronger spring bloom in the South Yellow Sea. Meanwhile, fast cooling might be responsible for the weak autumn blooms in the specific zones. Shoaling stratification driven by fast warming can maintain the rapid growth of phytoplankton due to the light and nutrient advantages in surface waters. A similar explanation is applicable for the impact of slow warming on the weak spring bloom. For different seasonal blooms, the bottom-up responses may vary spatially. For example, in the YS, the warming scenario

may intensify the warming/cooling rate in spring/autumn, promote an earlier spring bloom, further weaken the autumn bloom in the central area and probably enhance the magnitude of the winter bloom in the south zone (Song et al, 2018).

1.2N/P/Si changes

The concentration and composition of nutrients have an important impact on the growth and composition of phytoplankton community. In recent decades, human perturbations have significantly changed the nutrients structure in coastal waters, resulting in disproportionate nutrients ratios and ecological structure of coastal waters.

Numerous studies have been conducted on nutrients limitation. Redfield was the one of the first scientists to emphasize the relatively fixed composition of phytoplankton in the world's oceans, that is, the atomic ratio of C: N: P is 106:16:1. Therefore, the Redfield ratio is widely used to evaluate various marine environments. However, when the nutrients concentration approaches the detection limit, Redfield ratio proves not to be as effective. Therefore, some scholars have suggested that the lowest threshold of nutrients that can be utilized by phytoplankton should be determined first. Fisher *et al.* (1999) proposed that the limiting concentration of nutrient was $\text{DIN}=2 \mu\text{mol/L}$ and $\text{P}=0.2 \mu\text{mol/L}$. Nelson *et al.* (1990) proposed the lowest threshold for phytoplankton growth was $\text{Si}=2 \mu\text{mol/L}$, $\text{DIN}=1 \mu\text{mol/L}$ and $\text{P}=0.1 \mu\text{mol/L}$. Justic *et al.* (1995) proposed a systematic assessment of nutrient stoichiometric limit: (1) if $\text{Si: P}>22$, $\text{DIN:P}>22$, phosphate was the limiting factor; (2) if $\text{DIN:P}<10$, $\text{Si: DIN}>1$, nitrogen was the limiting factor; (3) If $\text{Si: P}<10$, $\text{Si: DIN}<1$, silicon was the limiting factor.

Composition of marine phytoplankton communities is affected by nutrients composition in the ocean. Escaravage (1996) showed that an increase in DIN/P would cause a corresponding decrease in primary productivity, which was more suitable for diatoms to become dominant species. When phosphorus limitation was transferred to silicon limitation, dinoflagellates replaced diatoms to become new dominant species. Billen (1985) proposed that high DIN/P gave rise to diatoms, and low DIN/P

contributed to the competitive advantage of dinoflagellates in German Bight Bay. Although the research results of different scholars were slightly different, the overall results showed that higher concentrations of nitrogen salts were beneficial to the growth of dinoflagellates, and silicates were beneficial to the growth of diatoms. When phosphorus limitation was transferred to silicon limitation, dinoflagellates replaced diatoms to become new dominant species.

1.2.1 Temporal variations of nutrients

The locations of survey stations in the southern Yellow Sea during 1950s to 2017 are shown in Fig. 1-14. The annual average changes in concentration of DIN, phosphate and silicate are shown in Fig. 1-14.

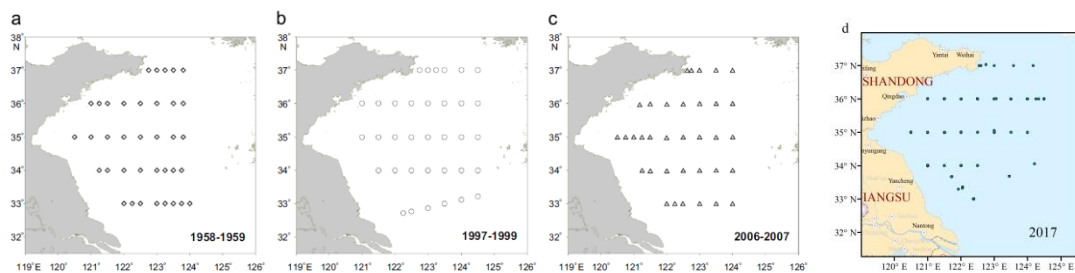


Fig. 1-14 Locations of survey stations in the southern Yellow Sea during different time periods.

From 1990s to 2017, DIN concentrations in the surface and bottom layer of the South Yellow Sea increased from 1990s to 2000s, and then ended up in decreasing from 2000s to 2017. DIN concentration was highest during 2006-2007, with an average concentration of 0.081 mg/L at the surface and 0.131 mg/L at the bottom.

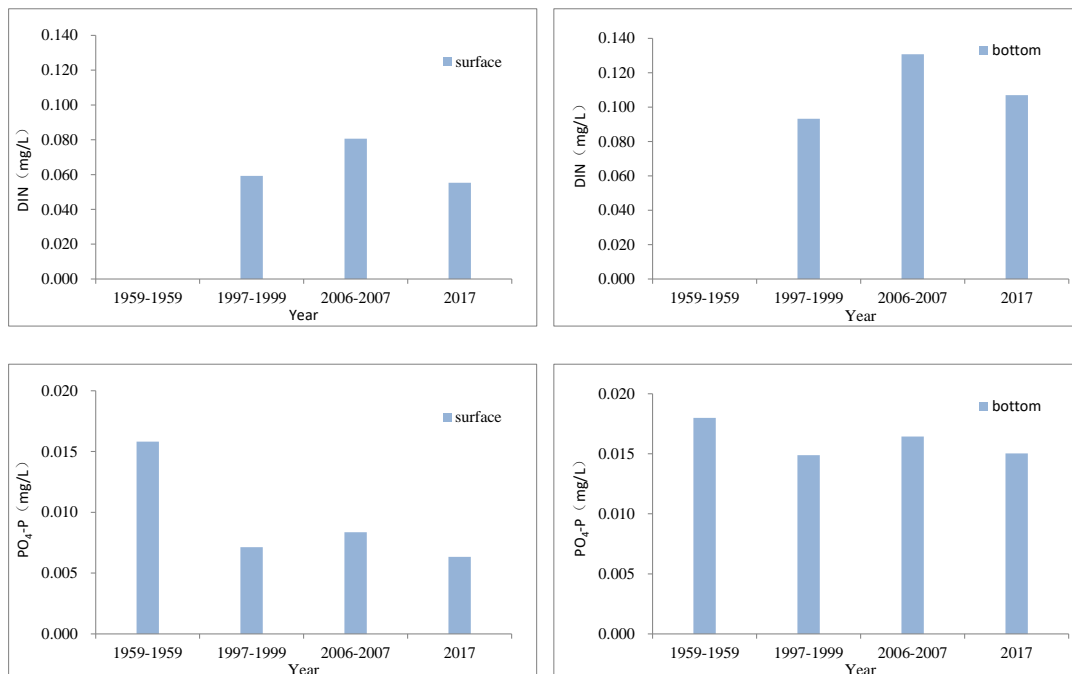
The surface and bottom concentration of phosphate exhibited a similar variation pattern, with the concentrations decreasing from 1950s to 2017. From 1990s to 2017, the average phosphate content remained relatively steady, with an average concentration of 0.007 mg/L at the surface and 0.015 mg/L at the bottom.

During 1950s to 2017, the concentration of silicate fluctuated dramatically. From 1950s to 1990s, the concentration decreased by nearly half, with 0.286 mg/L in 1950s and 0.141 mg/L in 1990s. From 1990s to 2000s, the concentration slightly increased to

0.172mg/L, and the concentration remained basically unchanged in recent years. Compared with the surface layer, the concentration of silicate at the bottom showed a similar pattern with surface layer. But the concentration of silicate at the bottom in 2017 was significantly higher than that of 1990s and 2000s.

1.2.2 Variations of nutrients structure.

The variations of nutrients structure in the southern Yellow Sea are analyzed during 1990s to 2017(Fig. 1-15). Table 1-3 shows the surface and bottom N/P ratio and Si/N ratio. Overall, the N/P ratio increased from 1990s to 2010s, with the surface N/P ratio increasing from 20.72 to 22.17 and the bottom N/P ratio increased from 13.95 to 22.17. The maximum surface N/P ratio (23.7) occurred in 2000s and the maximum bottom ratio (22.17) occurred in 2017. In 2017, the ratio of N/P was greater than the Redfield ratio (16:1). Si/N ratio decreased slightly to 1.08(surface) and 1.07(bottom) during 1990s to 2000s and then started to increase to 2.20(surface) and 1.76(bottom) in 2017.



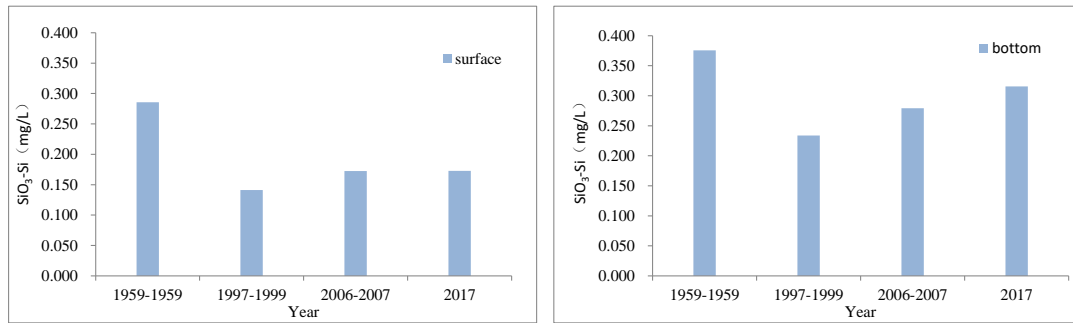


Fig. 1-15 Temporal variations in concentration of nutrients in the southern Yellow Sea during different periods.

Table 1-3 Temporal variations in nutrient ratios in the southern Yellow Sea during different periods.

Period	N: P		Si: N		literature
	surface	bottom	surface	bottom	
1997-1999	20.72	13.95	1.20	1.26	[2]
2006-2007	23.7	17.71	1.08	1.07	[2]
2017	22.17	22.17	2.20	1.76	

1.3 HABs (including drifting macroalgae)

1.3.1 Microalgae

Harmful algal bloom (HAB) is a term adopted by the Intergovernmental Oceanographic Commission (IOC) of UNESCO; it is internationally recognized to refer to any proliferation of microalgae (regardless of the concentration) perceived as harmful owing to its negative impact on public health, aquaculture, the environment and/or recreational activities.

The IOC Intergovernmental Panel on Harmful Algal Blooms (IPHAB) was formed at the Sixteenth Session of the IOC Assembly, March 1991, in order to identify adequate resources for a broad programme to try to solve some of the problems caused by harmful algae. And an international programme on Harmful Algal Blooms was

established by the Intergovernmental Oceanographic Commission (IOC) of UNESCO in 1992, with the overall objective to foster the effective management of, and scientific research on, harmful algal blooms in order to understand their causes, predict their occurrences, and mitigate their effects. Objectives have been expanded to develop and improve methods to minimize the environmental and economic consequences of harmful algae and to promote and facilitate the development and implementation of appropriate monitoring programmes, thereby to protect public health and ensure seafood quality.

In 2009, a 4-year IAEA TC project was initiated on Designing and Implementing Systems for Early Warning and Evaluation of the Toxicity of Harmful Algal Blooms in the Caribbean Region, Applying Advanced Nuclear Techniques, Radioecotoxicological Evaluations and Bioassays (ARCAL RLA/7/014) was established. Results from this project and its capacity development activities included the publication of a manual in Spanish to strengthen capacities to monitor HABs events and to mitigate their deleterious effects. This HABs manual was translated into English, and expanded with the addition of chapters related to benthic HAB species. This manual is intended as an introduction to basic analytical techniques that can be applied when designing a standard sampling protocol for both planktonic and benthic microalgae (and associated environmental conditions) and vectors of biotoxins (shellfish and fish). This standardization of methods will enable more robust data comparisons between countries and will yield improved risk assessments of potentially toxic HAB events.

The Global Ecology and Oceanography of Harmful Algal Blooms (GEOHAB) programme was initiated in 1999 by the Scientific Committee on Oceanic Research (SCOR) and the Intergovernmental Oceanographic Commission (IOC) of UNESCO to develop a research programme on the ecological and oceanographic mechanisms underlying the population dynamics of harmful algal blooms (HABs). The ultimate goal of this programme is to promote the development of observation systems and models that will enable prediction of HABs, thereby reducing their impacts on the health of humans and marine organisms, as well as economy and societies.

GEOHAB has adopted a 3-category system for defining and endorsing research.

Core Research is comparative, multidisciplinary, and international research, which directly addresses the overall goals of GEOHAB outlined in the Science Plan. Core research comprises oceanographic field studies, application of models, and comparable ecosystems, and it is supported by identification of relevant organisms, and measurements of the physical, chemical and biological processes that control their population dynamics. So far, GEOHAB has developed Core Research Project Reports on Upwelling Systems, Eutrophic Systems, and Stratified Systems.

Targeted Research addresses specific objectives outlined in the Science Plan. Targeted Research may include, but is not limited to, the development and comparison of specific models and observational systems, studies on the autecological, physiological, and genetic processes related to HAB, and studies on sub-grid formulations of physical, chemical and biological interactions affecting HAB. Targeted Research differs from Core Research in scope and scale. Whereas Core Research is expected to be comparative, integrative, and multifaceted, Targeted Research activities may be more tightly focused and directed to a research issue or element. It is expected that such research activities will facilitate wider and larger-scale studies.

Regional/National Projects are those research and monitoring activities relevant to the objectives of the Science Plan and which are coordinated at a regional or national level.

The Regional Comparative Programme on HAB in Asia is thus a Regional Project. GEOHAB Asia was developed through two workshops. The first workshop was established in Tokyo, Japan on Mar. 15 and 16, 2007, aiming to review HAB research activities in Asia, while the other workshop was founded in Nha Trang, Vietnam on Jan. 31 and Feb. 1, 2008 and more focused on identifying key questions and research components to work out a plan for cooperative research in the region.

1.3.2 Macroalgae

Macroalgal blooms are a kind of biological disaster caused by the explosive proliferation of seaweeds and accumulation in the shallow waters of the bay. The macroalgal blooms first appeared in the late 1960s, initially in Europe, and then frequently appeared in some economically developed regions such as the Americas, Oceania, and Asia. In Europe, Denmark's Roskilde Bay, the Dutch Weiss Sea Lagoon, France's Brittany, and even the famous Venice have all been invaded by large-scale macroalgal blooms. In Asia, Japan's Yokohama, Mikawa, Miyajima, and Kochi regions as well as South Korea and the Philippines are all frequented by macroalgae.

The emergence of the macroalgal blooms in China began at the end of the last century. Because of the small scale, it failed to attract attention. It was not until 2008 when a large-scale *Ulva* blooms broke out during Olympic sailing competition held in Qingdao that people finally realized the power and harm of the macroalgal blooms. In recent years, the area where green tides occur in China's seas has shown an obvious increase, and the types of macroalgal blooms have also diversified, such as *Mazaella* and *Sargassum* blooms in Xinghai bay of Dalian, *Ulva* blooms in Yantai and Xiamen, and *Sargassum* blooms in Guangxi.

Since 2015, Floating *Ulva* populations have occurred in Daludao island of Dandong, However, macroalgal bloom has not yet appeared in Haizhou Bay.

1.4 Jellyfish blooms

In recent years, the frequency and categories of marine ecological disasters have been increasing. Jellyfish blooms have become a new type of marine ecological disaster after red tide, green tide and other ecological disasters globally. Jellyfish disasters were formed by an abnormal increasing number of jellyfish in local waters, which undermined the safety of outdoor bathing place, and impacted the normal intake of industrial water and fishing seriously. Jellyfish bloom is a natural phenomenon, which blooms about every 40 years in history. However, the outbreak frequency is higher and higher to an alarming rate of once every one year in recent years. The outbreak of *Aurelia aurita* caused the fisheries production loss in Japan in 1950. In the 1960 s,

Aurelia aurita blocked coastal power plant circulating water system and for several times, and even resulted in the entire Japanese plants downtime. Such events have spread all over the world to the sea area in South Korea, India, Saudi Arabia, Philippines and Australian. Besides, Denmark, Greece, Britain and Norwegian have suffered remendous local economic loss because of the *Aurelia aurita* bloom.

Jellyfish disasters used to bloom occasionally and failed to attract peoples' attention before the middle of 1990s. Since offshore ecosystems have changed a lot in China under the pressure of the global temperature change, the increasing intensity of human activities and the overfishing of fishery resources, jellyfish disasters have become more frequent, with large outbreaks in the Bohai Sea, the northern East China Sea and the southern Yellow Sea. The frequency of jellyfish disasters in northern China is significantly higher than that in southern China. In recent years, the density of jellyfish in Bohai Sea has been on the rise, and local waters has seen significant increase in jellyfish bloom (Table 1-4). At present, the main giant species of jellyfish outbreak in China are *Aurelia aurita*, *Nemopilema nomurai*, and *Cyanea nozakii*. The biomass of small jellyfish (below 2cm), such as *Pleurobrachia globosa*, also increased.

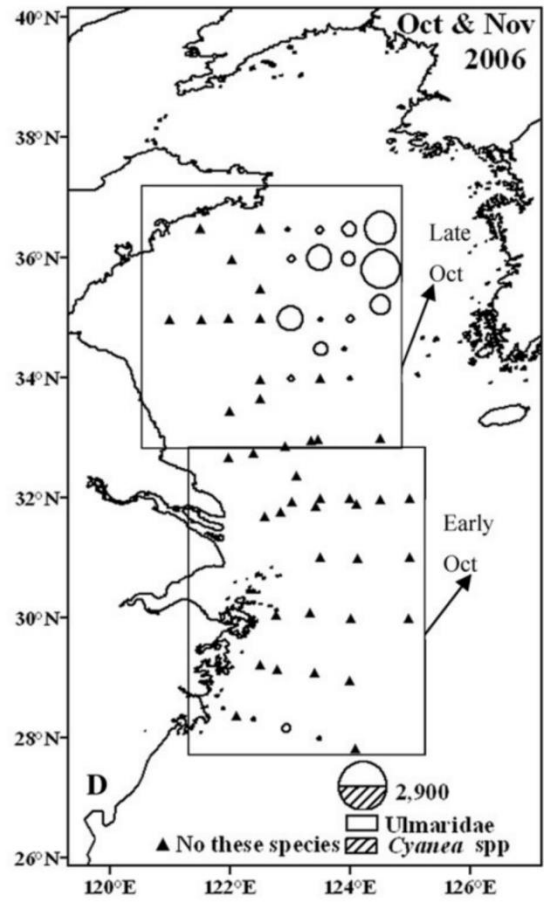
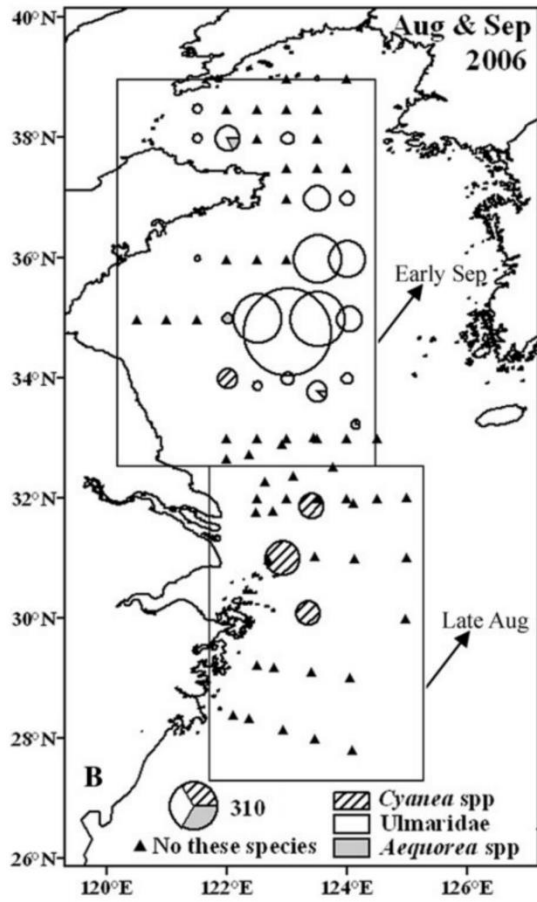
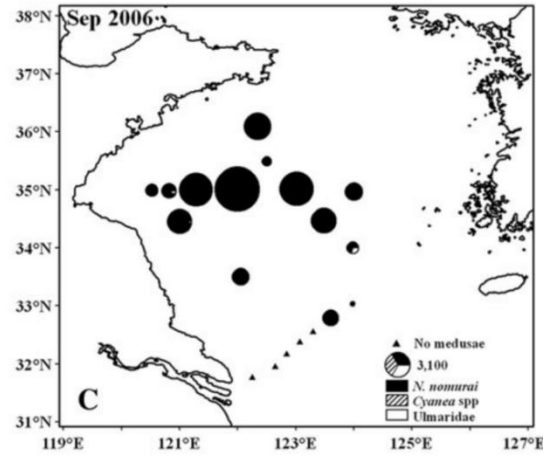
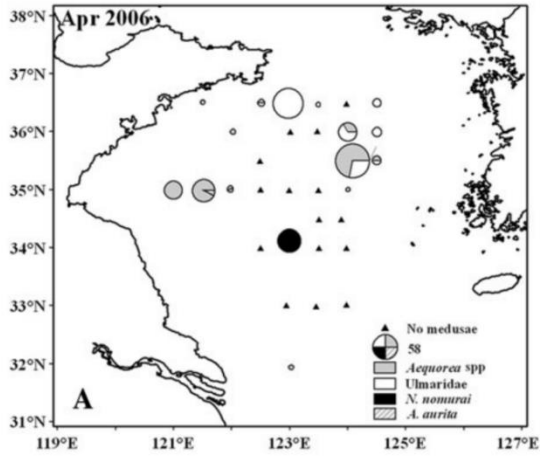
Table 1-4. Published accounts of jellyfish blooms in Chinese seas and their negative impacts on human enterprises (Dong et al., 2010).

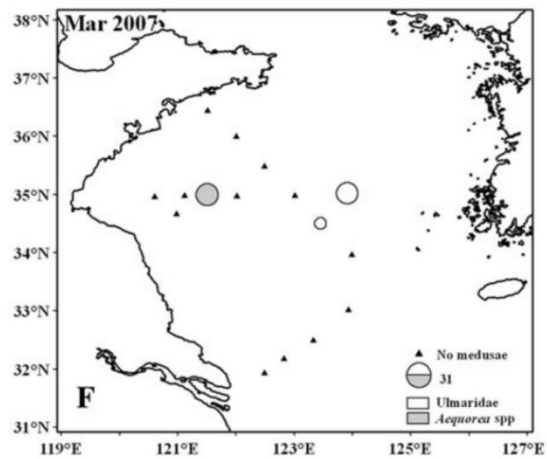
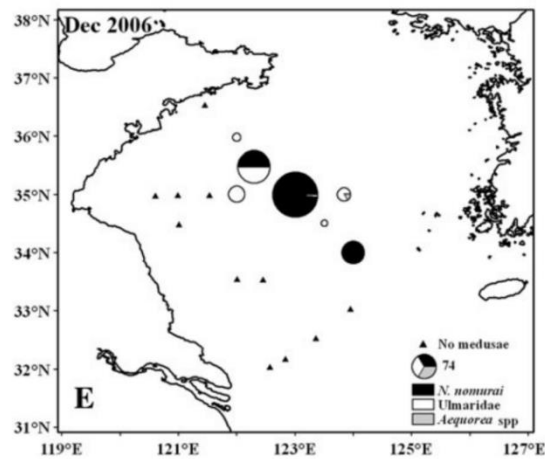
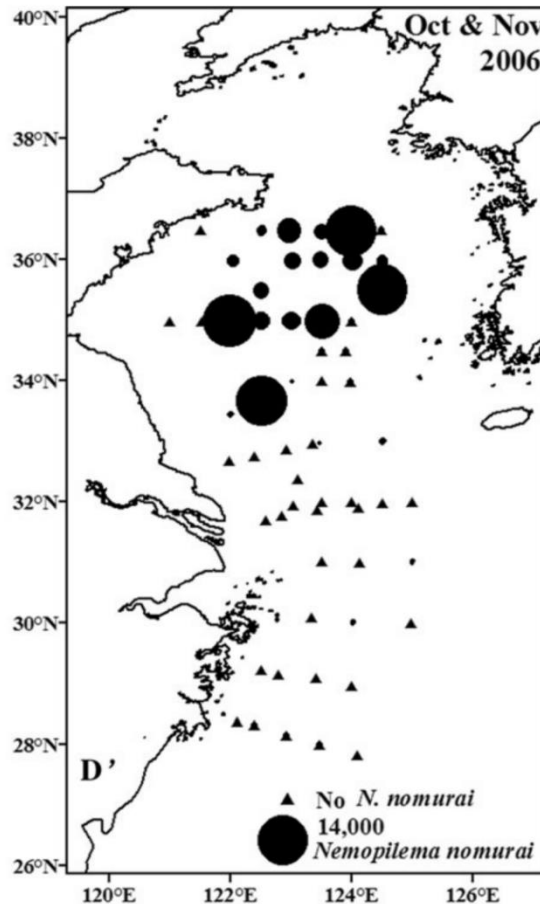
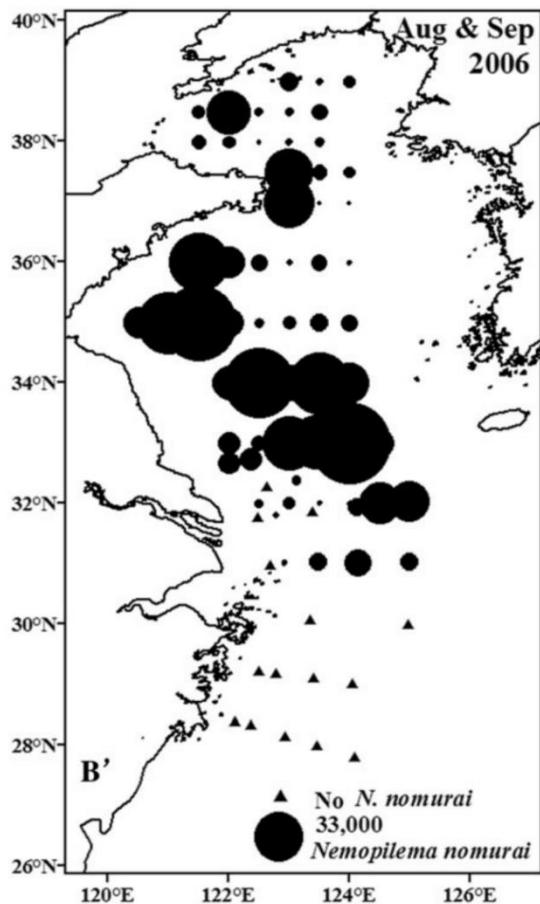
Species	Year	Location	Direct consequences
<i>Aurelia aurita</i>	2004; 2008	Qinhuangdao, Hebei province	Over 4000 tons of <i>A. aurita</i> were cleaned up in July 2008
<i>A. aurita</i>	2007	Yantai, Shandong province	Interference with aquaculture
<i>A. aurita</i>	2008	Weihai, Shandong province	20–50 tons of <i>A. aurita</i> were cleaned up each day
<i>A. aurita</i>	2009	Qingdao, Shandong province	Over 10 tons of <i>A. aurita</i> were cleaned up for two days
<i>Cyanea</i> sp.; <i>Nemopilema nomurai</i>	1999	Middle South Zhejiang province	Interference with fisheries
<i>Cyanea nozakii</i>	2004	Liaodong Bay	Sharp decline of edible jellyfish <i>Rhopilema esculentum</i>
<i>Cyanea</i> sp.	2003; 2004	Yangtze Estuary	Comprised 85.47% of the total catch of fisheries in November 2003 and 98.44% in May 2004
<i>Nemopilema nomurai</i>	2003–2005	East China sea	Mean biomass in monitoring sites 608–7144 kg/h
<i>N. nomurai</i>	2005; 2007	Huludao, Liaoning province	Interference with fisheries

From 2003 to 2014, there were several incidents of jellyfish blooms, causing blockages in the water intake of power plants, loss of offshore catches and injuries on beaches. In 2004, the abnormal proliferation of *Cyanea nozakii* in Liaodong Bay of

Bohai Sea was particularly significant, which resulted in the reduction of *Rhopilema esculentum* and fishing industry. From June to September 2007, a very rare bloom of *Aurelia aurita* occurred in the coastal areas in Yantai and Weihai, Shandong province. Since 2008, the coastal power plants in the north areas of Qingdao and Longkou have suffered from jellyfish boom for many years. In July 2009, the jellyfish bloom hit power plant in Qingdao and hampered the safe operation. In late July 2013, a high-density jellyfish population formed in the waters around the Hongyanhe nuclear power plant in Liaoning province. On July 21, 2014, the Hongyanhe nuclear power plant suffered an outage because *Aurelia aurita* blocked the cold water intake system. In the south of China, jellyfish invaded the cold water system of nuclear power in Daya Bay from February to March 2017. From 2003 to 2016, the average number of people stung by jellyfish on the beach was up to 1,400 per year, and the total number of deaths was 21. An eight-year-old boy was stung by *Nemopilema nomurai*, which caused acute pulmonary edema, and he died in rescue on August 2, 2013.

Blooms of giant jellyfish have formed increasingly in the southern Yellow Sea (YS) and northern East China Sea (ECS) during summer and fall since the end of the 1990s. The distribution of giant jellyfish varies with seasons, temperature, salinity and other hydrological conditions throughout the coastal waters in the southern YS and northern ECS. The distribution was mainly in the Yangtze Estuary and Subei shoal. Zhang et al. (2012) sampled giant jellyfishes using bottom trawl surveys during 2006–2007 in the YS and ECS. Bottom trawl surveys provided the first opportunity to sample giant jellyfish in the YS and ECS to assess population biomass and abundance over large areas and in different seasons. Distribution, biomass, and biomass composition of the jellyfish assemblage during April 2006 to August 2007 surveys in Chinese waters were shown in Fig. 1-16. Wei et al. (2015) described the observation of distribution of *N. nomurai* made on R/V Beidou from July to August, 2009 (Fig. 1-17). Most medusas were observed gathering between the 30 m and 50 m isobaths near the tidal front to the south of the Shandong Peninsular. All stations with *N. nomurai* abundance exceeding 1.0×10^4 ind./km² were located in the tidal front area.





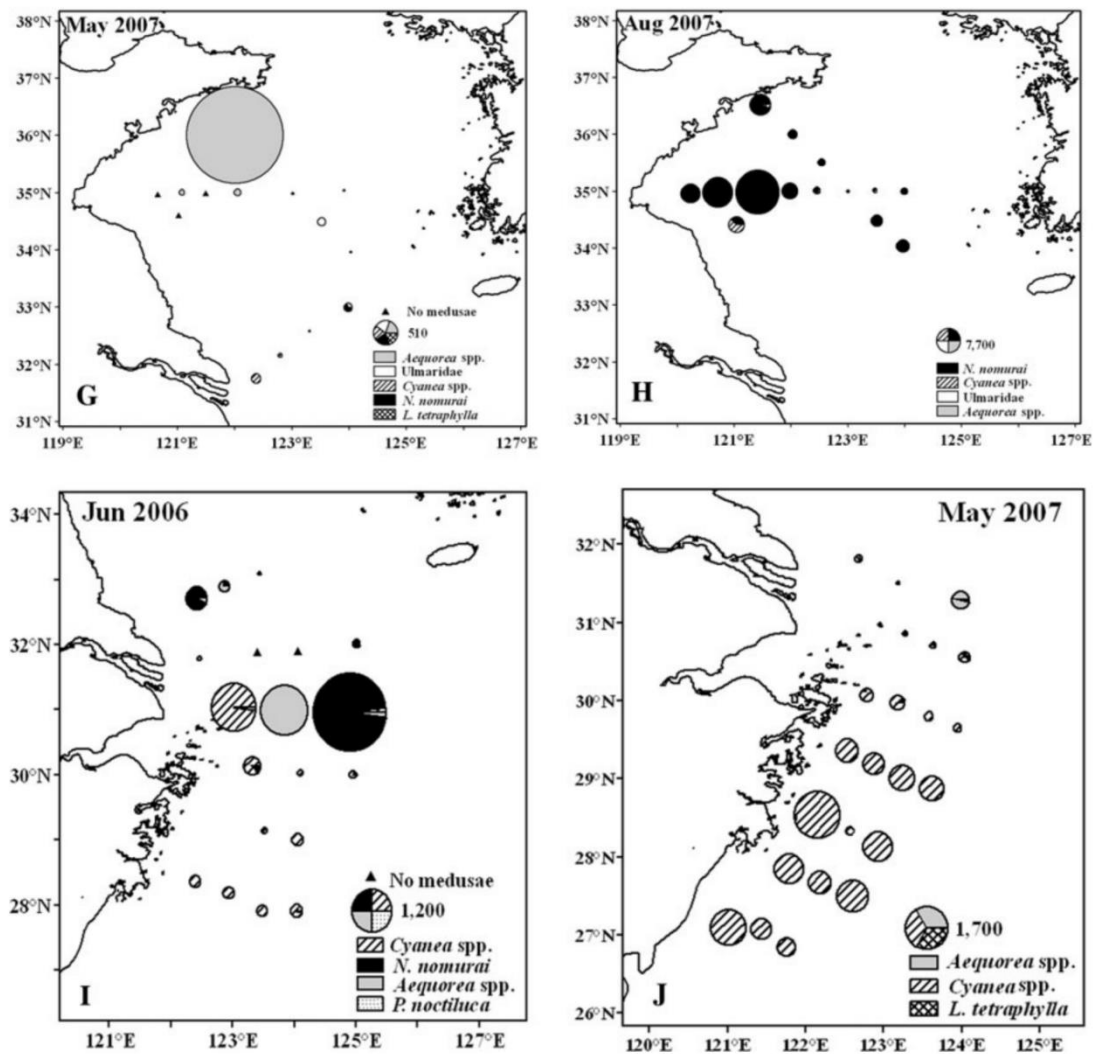


Figure 1-16. Distribution, biomass, and biomass composition of the jellyfish assemblage during April 2006 to August 2007 surveys in Chinese waters.

A–J Pies indicate total jellyfish biomass (pie size: biomass, kg km^{-2} . Biomass increases linearly with the pie area at each station), different shadings indicate different jellyfish species, with proportions as percentages of the pie area. Note that in (B) and (D), biomass of *Nemopilema nomurai* was excluded to show biomasses of other species, which otherwise would be masked by *N. nomurai* due to their huge biomass. The biomass of *N. nomurai* was shown instead in (B') and (D'). Different scale bars used for different surveys. *A. aurita* = *Aurelia aurita*; *L. tetraphylla* = *Liriope tetraphylla*; *P. noctiluca* = *Pelagia noctiluca*.

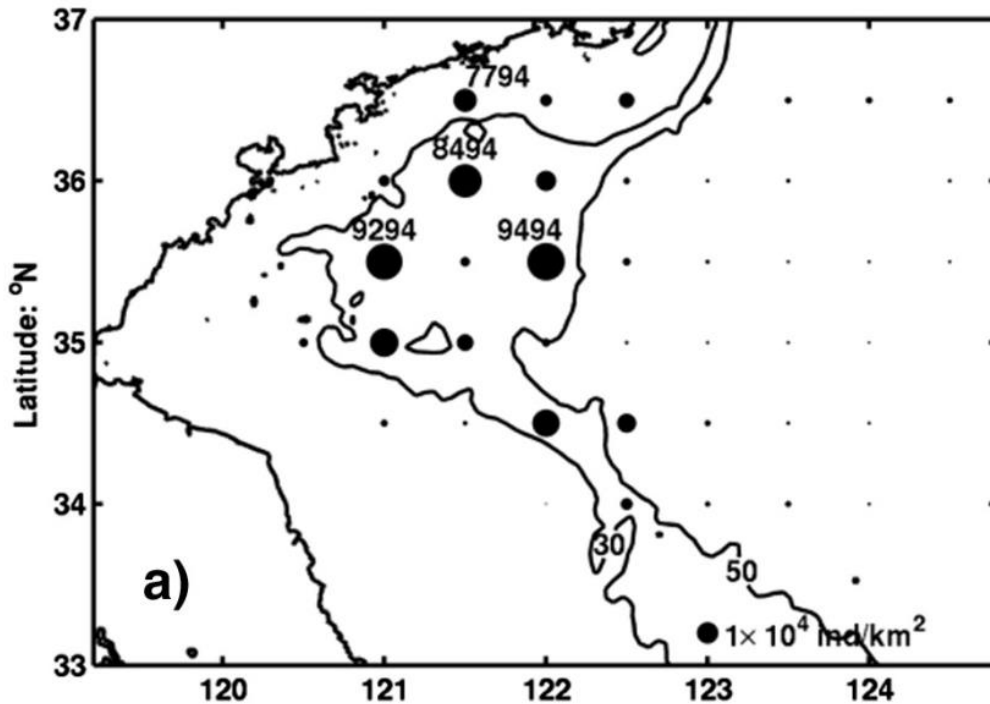


Figure 1-17. Observed distributions of *N. nomurai* in early August, 2009. Observations were made from July 29 to August 7. The station numbers of observations are denoted. Contour lines are water depth. Solid dots represent the abundance.

Currently, there is no unified method for the abundance or biomass estimation of the giant jellyfish, and it is generally believed that the quantification of giant jellyfish is difficult. The common problem is that giant jellyfish have large water content, large volume, and patch distribution, which all lead to inaccurate biomass estimation. Among traditional methods of netting, acoustics, optics and imaging systems, imaging systems are more widely used. The traditional investigation method using plankton trawl was to evaluate the bottom trawl fisheries resource.

When evaluating the biomass and abundance of jellyfish species, although the current method was semi-quantitative method in some extent, the method of relative indexes as quantitative biomass of inter-annual comparison was of practical significance according to the use of historical data of jellyfish abundance. The use of netting tools, such as bottom trawling, may lead to underestimation of biomass or

abundance. One reason is that the opening widths of the nets will change under variable water pressure, making it difficult to quantify. Another is the vertical and horizontal distribution of patches on jellyfish. For example, it was reported that the distribution of jellyfish in the south of the North Sea was mainly in the range of 5-25m, which was not evenly distributed in the vertical direction. In the normal investigation of the Yellow sea in China, large amounts of jellyfish were also found in the surface or subsurface of many stations, and the sand jellyfish in the southern part of Japan Sea mainly accumulated in the water layer above 40m. Thirdly, the type of netting, including middle net or bottom trawl, cannot fully capture all of jellyfish except the target water layer set by the netting. Therefore, it is necessary to estimate the capture efficiency or catch rate.

Including the traditional netting method for measuring jellyfish abundance, the method called sight survey for visually counting giant jellyfish abundance on the ship's deck has been also used by many scientists. Since 2006, the research group of professor Uye of Hiroshima University has been carrying out sight survey on ferry boats from the surrounding cities of Japan Sea to the surrounding cities of the East China Sea to number the distribution and abundance of giant jellyfish in the surface of Yellow Sea and Japan Sea by sighting. The advantage of the sight survey method is that it is easy to operate, economical and labor-saving. The disadvantage is that the abundance of jellyfish can only be observed on the surface of water or in the upper water. The use of this method is affected by weather, hydrological conditions, vertical movement behavior of jellyfish, etc. Therefore, quantitative monitoring by this method is not entirely accurate. Sight survey was rarely reported and was only done by research ships rather than by ferry boats in China. Wang *et al.* observed a bloom of jellyfish (*Aequorea* spp.) during a comprehensive investigation in the Yellow and East China Seas in April 2011.

In order to illustrate the geographical variations in abundance, size, and biomass, sight survey by naked eyes was carried out at each station. A plankton net was used to collect jellyfish samples and calculate their abundance. The researchers stood on the

back deck when the ship stopped. Their eyes were about 4m above the sea surface, the furthest distance of observation was about 10m, the observation was maintained 30 minutes, and the number of surface multi-tube jellyfish within their visual range was measured and recorded. The results showed that the occurrence frequency of the dark green multi-tube jellyfish was 16% in all stations, mainly in the south coast of the East China Sea. During August 1 to September 30, 2011, the population abundances and distributions of three scyphozoan jellyfish species *Nemopelima nomurai*, *Cyanea nozakii* and *Aurelia aurita* were examined by visual observation twice per week by Wang Shiwei *et al.* The researchers divided the observers into two groups, standing on both sides of the bow of the survey ship, the speed of which was 6 knots. During the course of the voyage, a unit of time was set at 5 minutes, the total number of jellyfish observed in the field of vision was counted, and longitude and latitude were recorded synchronously.

The specific calculation method of average abundance of jellyfish was as follows: During the period of stopping for related visual verification, the results showed that in the visual range of bow standing, W_0 which could distinguish the jellyfish's biggest observed distance was 20m (10m each side). Assuming that the total voyage distance was D , then the total observed area was $A = W_0D$. If the total number of giant jellyfish observed was N_0 , and the average abundance of this species during observation was $M = N_0/A = N_0/(W_0D)$. Because each observation route covered most of the water in the bay, M was used to represent the average abundance of jellyfish in the bay. According to the results, *Aurelia aurita* showed a trend of gradual decline.

The populations of both *Nemopelima nomurai* and *Cyanea nozakii* reached their peak on August 11, and declined successively at the end of August and the middle of September. At the end of September, three kinds of jellyfish had basically disappeared. At present, there are only two reports about using visual method to monitor jellyfish, which is still not widely used, possibly because the marine survey in China is mainly carried out by research ships. Most jellyfish surveys do not use visual methods because of its time limitations. Future studies are expected to be carried out on more ferry

voyages and use visual methods to monitor giant jellyfish in a wider area of the ocean in order to collect more data.

Including sight survey and trawl net, Lynam used acoustics to assess jellyfish biomass in Benguela Sea, Namibia. Scientists from Swansea University in UK and Irish established the first jellyfish tracking project (EcoJel) to keep track of the movement of jellyfish along the coast of South Welsh by using small electronic tracking markers. Based on the research of jellyfish species, toxicity and jellyfish monitoring system in the waters near Jeju Island in Korea, jellyfish monitoring system was formally established in 2011 to provide information for predicting the trend of jellyfish movement, release water quality status of sea baths, and select locations for fishing boat operation. And in July 2014, the integrated control system for automatic detection and removal of jellyfish using intelligent robots was put into trial operation. By means of ship monitoring, remote sensing monitoring, buoy monitoring, fishery market survey and other diversified means, Japan can obtain the distribution of giant jellyfish in the monitoring sea area at any time. After summarizing and forecasting, it is processed as real-time visualized jellyfish distribution and forecasting information. Finally, it is timely released to fishermen and other people whose work is related to sea. And it is possible to organize relevant departments responsible to remove giant jellyfish, effectively reducing the loss of jellyfish disaster. NOAA and several universities in the United States have developed a long-term prediction system for the occurrence of Pacific gold jellyfish, and regularly issued early warning bulletins for jellyfish. Based on jellyfish drift patterns and monitoring results of Berline in 2012, the Marine Laboratory of Free City along the Coast of France launched a 48-hour online jellyfish early warning system for coastal beaches from Marseille to Muntou and from St Tropez to the Italian border, and published jellyfish forecasting and grading alerts on two websites of “jellywatch” and “Medazur”. China has developed rapid quantitative monitoring of harmful species, drift path prediction, early warning of disaster risk level and emergency disposal technology of jellyfish disasters, constructed a jellyfish disaster monitoring and early warning technology system, and carried out demonstration of the

application in typical waters of jellyfish disasters such as Qingdao offshore, Qinhuangdao and Xiamen.

Yang Dongfang *et al.* analyzed the application of new technologies (underwater photography, sonar imaging and aerial imaging) of jellyfish monitoring methods in recent years, and compared the advantages and disadvantages of various monitoring methods, which made a useful supplement for the comprehensive understanding of jellyfish monitoring methods. The advantage of underwater camera monitoring method was that it had high resolution and could reflect the movement behavior of jellyfish, and the temporal and spatial distribution, movement process and behavior performance of jellyfish could be recorded by underwater camera. Its disadvantage was that the field of vision was limited. In recent years, the underwater camera technology had been constantly improved in the process of development with the resolution and the scope of monitoring constantly expanding.

The advantages of the sonar imaging monitoring method included wide monitoring range, the ability to monitor both the horizontal and vertical distribution of jellyfish, and the ability to monitor in muddy or dim water. The disadvantages lie in low resolution, the inability to distinguish species from species, and the inability to reflect the movement of jellyfish. In recent years, a combination of acoustic and optical image has been developed for the quantitative detection of jellyfish. Aerial images, on the surface or near surface, can observe the distribution, movement and behavior of giant jellyfish. Another advantage of aerial surveillance was that it could make these observations without disturbing the jellyfish.

2. Regional monitoring system

2.1 Sampling regions

According to the HABs monitoring data, most HABs events were reported in coastal waters of Donggang and Haizhou bay, and the data of N/P/Si changes also have been analyzed in these two areas in a long term. So the two coastal waters of Donggang and Haizhou bay were suggested as the sampling regions in YS of China side, although there are no blooms of jellyfish historically. We suggest setting three sections, and establishing five stations for each section. Five nautical miles between two stations is suggested.

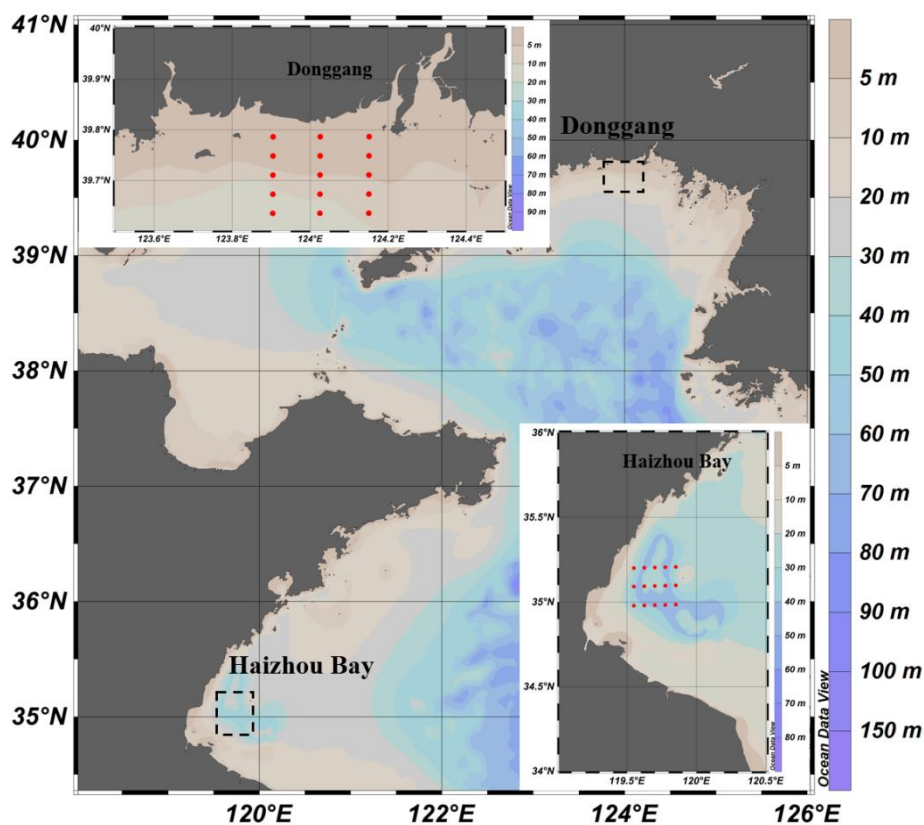


Fig. 2-1 Suggested schematic diagram of sampling locations of China side.

2.2 Sampling period

Most HABs events occurred from May to September every year; and jellyfish

ephyra occurred in May, larvae occurred from May to June, medusa blooms usually from July to August every year in usual. Therefore, we recommend setting sampling time from May to August, and the sampling frequency is once a month.

2.3 Sampling methods

Nutrient, phytoplankton and jellyfish are sampled by gear net at each station from May to August, and jellyfish is also monitored by sight survey during the voyage between stations and some ferry lines (Fig. 2.3-2) when it blooms from July to August. The specific monitoring methods are as follows.

2.3.1 Climate change

1) Monitoring elements

Sea surface temperature, chlorophyll.

2) Standard methods

The two monitoring elements both can be determined by YSI.

2.3.2 N/P/Si changes

1) Monitoring elements

Nitrite, nitrate, ammonia, phosphate and silicate.

2) Standard methods

Pretreatment: The sample was filtered through a 0.45 μm cellulose acetate membrane, then frozen and stored at -20 °C.

Nitrite: It can be determined by Diazo-azo reaction. Nitrite reacts with an amine to form a diazonium salt which in turn could be coupled with a second amine to form an azo dye.

Nitrate: It can be determined by copper-cadmium column reduction and Diazo-azo reaction. The same method was used to nitrate in seawater after reduction of nitrate to nitrite by copper-cadmium column.

Ammonia: Hypobromate oxidation. The same method was also used to determine

ammonia in seawater after the oxidation of ammonia to nitrite by bromate.

Phosphate: phosphomolybdate blue spectrophotometry.

Silicate: silicon-molybdenum blue spectrophotometry.

2.3.3 HABs

1) Microalgae Sampling

Bottle sampling can be deployed from almost any vessel, and it gives an accurate quantitative assessment of species densities within the depth sampled. Fixed depth sampling (e.g. 0, 10, 20 m, and a near sea floor sample,) can be informative.

Plankton nets can also be used to sample the phytoplankton community, but this type of collection is not quantitative.

a) Water sampling

At each station, water samples are taken for subsequent measurement of physical features (temperature and salinity), chemical features (dissolved oxygen, chemical oxygen demand, biological oxygen demand), nutrient (such as ammonia, nitrite, dissolved inorganic phosphate, reactive silicate, total phosphorus and total nitrogen), and trace metals (Cd, Cu, Co, Fe, Ni, Pb, Zn).

The recommended monitoring parameters are listed in Table 2.2-1.

Table 2.3-1 The recommended monitoring parameter for HAB monitoring.

Monitoring parameter			
HAB	Environmental parameter	Physical parameter	Meteorology
Type of HAB spp.	DO	Water temp.	Weather
Cell concentration	COD	Salinity	Wind direction/speed
Water color	Chlorophyll-a	Transparency	

	Nutrients		
	Trace metals		

b) Fixation procedures for microalgae samples

There are a number of different fixation methods for phytoplankton, but for routine monitoring programs, Lugol's is the preferred preservative. Acid Lugol's is made by dissolving 100 g potassium iodide (KI) in 1L of distilled water, then 50 g crystalline iodine (I₂) is dissolved in this solution followed by the addition of 100 mL of glacial acetic acid. This produces a 3% solution. For neutral Lugol's, the acid is omitted. For field samples, add 10 drops per 200 mL of sample.

c) Measurement in lab

To identify and to determine the abundance of phytoplankton, cells are typically counted under a microscope or using automated cell counters. The unit for abundance is usually cells per liter (cells/L) or cells per milliliter (cells/mL). To determine the abundance of harmful organisms and the biodiversity of samples, organisms should be identified to the species level if possible.

2) Macroalgae sampling

a) Intertidal zone

Surveys of intertidal zones are conducted on rocky shores, embankments or soft-sediment tidal flats with green algae, where at least three survey transections are generally set. At each transection, two stations are usually set up in the high tide area, three stations in the middle tide area, and one or two stations in the low tide area. In the short intertidal zone on the beach, one station is set up in the high tide area, three stations in the middle tide area, and one station in the low tide area.

b) Cultivation rafts

In each cultivation area, three breeding rafts are selected as three transections, three stations for each transection, and no less than two samples for each station.

c) **Biological sampling**

A 25 cm x 25 cm or 10 cm x 10 cm quadrat is used for sampling in intertidal zone. At each station, at least two samples are collected. After photographing, all the green algae in quadrat are sampled with shovel or rake, and saved in sample bags for further measurement of species richness, number and biomass. In cultivation area, quantitative sampling with a length of 10 cm is carried out on bamboo poles or cultivations ropes. All the green algae were collected as described above. The equipment used to perform the sampling include iron quadrat, collection bottle, collecting knife and tweezers etc.

Information centers could be set up in China and RO Korea respectively to share the information on the occurrence of HABs including drifting macroalgae blooms through the remote sensing and other monitoring means. China and Korea should work together to establish the monitoring network of HABs including drifting macroalgae.

2.3.4 Jellyfish

Plankton nets are recommended to sample jellyfish ephyra and larvae. And the anchor drift net is a better choice for medusa monitoring in the coastal waters. Such net has been practically used for four years at regions adjacent to Hongyanhe by Guan Chunjiang *et al*, and the effect of sampling was demonstrated in Fig. 2.1.

Sight survey (Modified from sighting survey method using ship of opportunity of Yoon *et al*, 2018) is easy to operate, economical and labor-saving. And it is more applicable for offshore areas, especially a vast area; And the cruise line depends on ferry route. The current cruise line covers “Incheon → Yantai → Dalian → Bayuquan → Incheon ” by Wonduk Yoon from Korea which has already been in operation, and one or two trips are advised to be introduced from Dalian to Nagasaki (an alternative, Fukuoka) in August and September (Fig. 2.3-2).

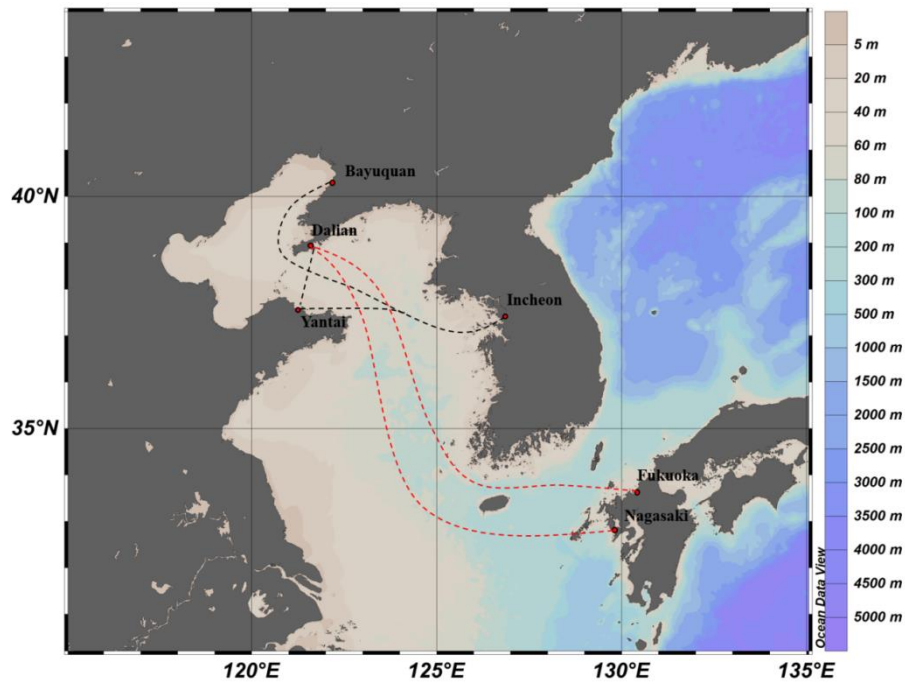


Fig. 2-2 The sight survey route map in YS

1) Net gear

The anchor drift net is a better choice for medusa monitoring in coastal waters. Such net has been practically used for four years at regions adjacent to Hongyanhe by Guan Chunjiang *et al*, and the sampling proves to be effective. The net is single-chip jellyfish anchor drift net, which is a kind of long band net composed of rectangle net chip. The height and length of the net is 8 m and 60 m, respectively, the mesh is 10 cm. The direction of net chip and ocean current should be vertical, and the net coupled with ocean currents should be drawn. Monitoring time is often at one-hour's interval.

2) Sight survey

First, the place for jellyfish monitoring should be chosen to measure the height (H) from the sea surface to the place of monitoring using laser rangefinder or tapeline, or string with marked meters. After setting sail, the GPS should be turned on to record geographical position and time. During cruise at steady speed of ship, the goniometer is used to measure the angle (a, between the ship and the foam). The width of foam can be estimated(P):

$$\tan (a) = \text{width of foam (P)} / \text{height (H)}$$

Calculate angle b:

$$\tan(b) = (P+10 \text{ m})/H.$$

If the situation is not favorable, or there are too many jellyfish in the 10 m width, we suggest decreasing the width to 5 m to make it easy to count. X (monitoring width) will be estimated. The amount of jellyfish will be counted every 5 minutes from dawn to sunset or from departure to arrival at port.

After cruise, such data as 5 min's distance (from GPS data), monitored surface with monitoring width, and jellyfish density in individuals in 100 m^{-2} will be estimated. Histogram figure will be worked out and put in a map.

3) Expressive methods of jellyfish biomass

For net gear, species name, abundance and diameter for every species should be recorded. Monitoring results should be expressed using ind/(net.h), jellyfish number/ (per net. per hour); or kg/(net.h), jellyfish weight/ (per net. per hour).

For sight survey, GPS data and the number of jellyfish should be recorded every 5min. Monitoring results should be expressed using ind/100m², jellyfish number/every 100m².

3. Discussion and strategies for development of regional monitoring system

This program gives a general introduction and detailed methods for monitoring N/P/Si changes, climate change, HABs (including drifting macroalgae), and jellyfish blooms. Though the sampling waters setting did not include Korea side, sampling stations could be set based on this program, and details vary from the specific situations for different regions. In view of this, in consideration of the development strategy of regional monitoring system, we suggest that, own and public regional monitoring areas of different monitoring objects for a long time should be set up in China and RO Korea according to the regional characteristics of different indicators (climate change, N/P/Si change, jellyfish blooms and HABs). Cooperation in the public areas should be strengthened. Shared voyage should be established to carry out a joint investigation. One or two long-term monitoring areas of all indicators should be set up to monitored and managed. The monitoring and management plan of the national and public monitoring areas should be subject to unified standards upon agreement by both sides. The relationship of environment changes and marine organisms has not been clear yet by the historical data. Long-term monitoring is required in the future.

Sight survey is a good method, and we believe that the anchor drift net is a suitable revision of other methods. We recommend that the anchor drift net is a better choice for medusa monitoring in coastal waters. Because the Bohai Sea is the continental sea of China, the ship route which include ports in the Bohai Sea should not be allowed by the government. The future research will not include any details in the Bohai Sea. There was only two ferry routes to Yantai and Weihai from Dalian, so we consider that the Yingkou station in the Bohai Sea should not be involved, and the route just end in Dalian.

The high biomass of jellyfish occurred between the sea of China and the Korean Peninsula: the Bohai Sea, YS and the north coast of the ECS. Many places in the east and west coasts of the YS were potential headstreams for Korea, so we could not ensure

the specific place and need to discuss deeply. Moreover, some researchers in Japan have pointed out that the increasing temperature of the early summer caused the hydra to jellyfish larvae (the 2-3mm), which reached the coast of Japan along the current (weighing 100kg) (上真一, 2005). The jellyfish were mature in April every year along the north of the Yangtze River and reached to Japan along the warm current. They were always seen in Japan from September to December (益田玲爾, 2006). Besides, the density of jellyfish in the middle of the YS was higher than that in coastal waters according to the investigation of jellyfish larvae in the middle of the yellow sea in the ECS, which proved the possibility that the place where the jellyfish occur was offshore (河原正人, 2006). Some researchers considered that the source of jellyfish in Korea is in the Bohai Sea, if are there some details about advection path and time?

A few ephyrae, metephyrae and juvenile medusae of this species first appear in China and Korea coastal sea areas in May and June. They first appear offshore of the Changjiang River, then are found successively in other northern sea areas: southwest of Cheju Island, the eastern coastal sea of Korea, the offshore of Gunsan, Korea. We suggested that some long-term monitoring stations or areas can be selected in Korea.

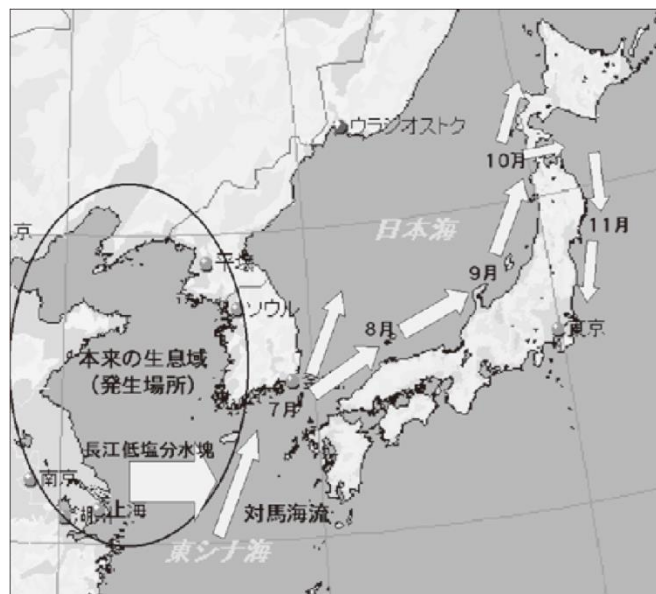


Fig. 3-1 Drift path of *N. nomuri* in Japan in 2006 (河原正人, 2006)

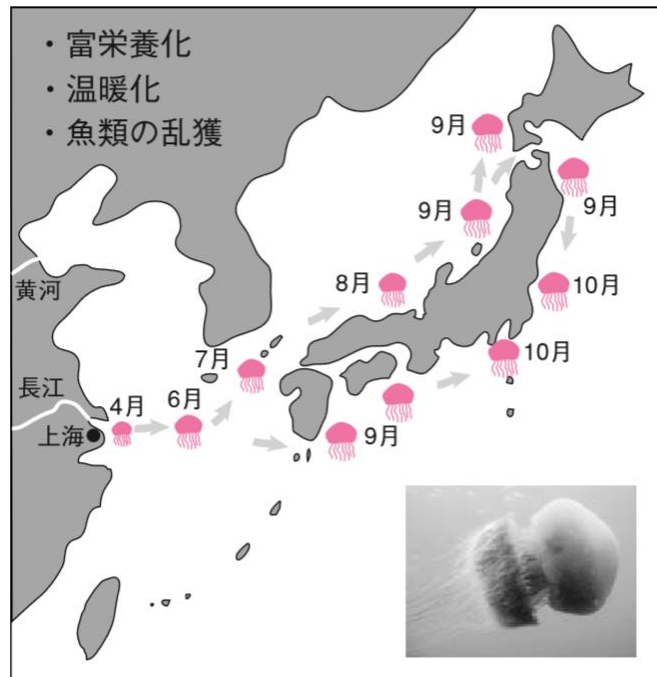


Fig. 3-2 Drift path of *N. nomuri* bloom in Japan in 2005 (益田玲爾, 2006)

4. References

- Dong Z., D. Liu, J. K. Keesing. 2010. Jellyfish blooms in China: dominant species, causes and consequences. *Marine Pollution Bulletin*, 60 (7), 954–963.
- Billen G M, 1985. A nitrogen budget of the Scheldt hydrographical basin. *Neth J Sea Res*, 19: 54 223~230.
- Escaravage S D, 1996. Response of phytoplankton communities to phosphorus input reduction in mesocosm experiments. *J Exp Mar Biol Ecol*, 188(1):55~79.
- Fisher, T.R.*et al.*, 1999. Spatial and temporal variation of resource limitation in Chesapeake Bay. *Marine Biology*, 133, 763-778.
- Lin C, Ning X, Su J, *et al.* 2005. Environmental changes and the responses of the ecosystems of the Yellow Sea during 1976–2000. *Journal of Marine Systems*, 55(3): 223-234.
- Liu P., Song H., Wang X., Wang Z., Pu X., Zhu M. 2012. Seasonal variability of the zooplankton community in the southwest of Huanghai Sea (Yellow Sea) Cold Water Mass. *Acta Oceanologica Sinica*, 31(4):127-139.
- Justic D, Rabalais N N, Turner R E, *et al*, 1995. Changes in nutrient structure of river -dominated coastal waters: stoichiometric nutrient balance and its consequences. *Estuarine, Coastal and Shelf Science*, 40: 339-356.
- Montagnes D J, Franklin D J, 2001. Effect of temperature on diatom volume, growth rate, and

- carbon and nitrogen content: reconsidering some paradigms. *Limnology and Oceanography* 46, 2008–2018.
- Nelson D M, Treguer P, Brzezinski M A, *et al*, 1995. Production and dissolution of biogenic silica in the ocean: revised global estimates, comparison with regional data and relationship to biogenic sedimentation. *Global Biogeochemistry Cycle*, 9: 359~372
- Park S, Chu P C, Lee J. 2011. Interannual-to-interdecadal variability of the Yellow Sea Cold Water Mass in 1967-2008: Characteristics and seasonal forcings. *Journal of Marine Systems*, 87(3-4):177-193.
- Song H, Ji R, Xin M, *et al*. 2018. Spatial heterogeneity of seasonal phytoplankton blooms in a marginal sea: physical drivers and biological responses. *ICES Journal of Marine Science* (submitted)
- UNDP/GEF. 2011. Seasonal variation of the major environmental parameters in the Yellow Sea Basin. UNDP/GEF Yellow Sea Project, Ansan, Republic of Korea (102 pages).
- Wang Y T, Sun S, Wang S W, *et al*. 2011. Geographical variations in abundance and size of (*Aequorea coerulescens*) in the Yellow and east China seas in spring. *Oceanologia Et Limnologia Sinica*, 42(6):1096-1102
- Wei H, Deng L, Wang Y, *et al*. 2015. Giant jellyfish *Nemopilema nomurai* gathering in the Yellow Sea—a numerical study. *Journal of Marine Systems*, 144: 107-116.
- YANG D F, CUI W L, ZHANG H L, *et al*. 2014. Application of new technology in jellyfish monitoring[J]. *Ocean Development and Management*, 31(4): 38-41.
- Zhang F, Sun S, Jin X, Li C. 2012. Associations of large jellyfish distributions with temperature and salinity in the Yellow Sea and East China Sea. *Hydrobiologia*, 690:81-96
- 上真一. 2005.エチゼンクラゲ海からの警告.
- 益田玲爾, 2006. 巨大エチゼンクラゲ—どこから来て、どこへ行くのか—
- 河原正人. 2006. 巨大エチゼンクラゲの大量出現機構の解明に関する生態学的・環境科学的研究. *食生活科学・文化及び環境に関する研究助成研究紀要*, 21: 131-138.